

Article

Aspirin Exerts Synergistic Effect with Anti-Fas Stimulation against Colorectal Cancer Stem Cells In Vitro

Magdalena Szaryńska^{1,*}, Agata Olejniczak-Kęder¹, Adrian Zubrzycki¹, Anna Wardowska² 
and Zbigniew Kmiec¹

¹ Department of Histology, Medical University of Gdansk, 80-210 Gdansk, Poland; agata.olejniczak-keder@gumed.edu.pl (A.O.-K.); adrian.zubrzycki@gumed.edu.pl (A.Z.); zbigniew.kmiec@gumed.edu.pl (Z.K.)

² Department of Physiopathology, Medical University of Gdansk, 80-210 Gdansk, Poland; anna.wardowska@gumed.edu.pl

* Correspondence: mszarynska@gumed.edu.pl; Tel.: +48-58-349-14-37

Abstract: Cancer cells, especially cancer stem cells (CSCs), are known for their therapeutic resistance and ability to induce a cancer relapse even many years after successful treatment. The quest for a novel protocol utilizing some commonly used non-oncologic drugs that would improve patients outcomes seems to be the right solution. Aspirin (ASA) is one of such eminent drugs. Our study demonstrated that ASA may exert synergistic effect with the anti-Fas antibody on CSCs of colorectal cancer cell lines. We found that such compound treatment inhibited the pro-cancerous effect of anti-Fas stimulation and decreased spherogenicity, survival and CD133-positive cells' count. Additionally, ASA with anti-Fas antibody may have a positive impact on dendritic cells' functions. Our innovative study explored simultaneous usage of two biologically active compounds which haven't been considered in such combination to assess their significance in colorectal cancer cell biology.

Keywords: cancer stem cells; colorectal cancer; anti-Fas; aspirin; dendritic cells



Citation: Szaryńska, M.; Olejniczak-Kęder, A.; Zubrzycki, A.; Wardowska, A.; Kmiec, Z. Aspirin Exerts Synergistic Effect with Anti-Fas Stimulation against Colorectal Cancer Stem Cells In Vitro. *Appl. Sci.* **2021**, *11*, 10009. <https://doi.org/10.3390/app112110009>

Academic Editor: Qi-Huang Zheng

Received: 26 August 2021

Accepted: 22 October 2021

Published: 26 October 2021

Publisher's Note: MDPI stays neutral with regard to jurisdictional claims in published maps and institutional affiliations.



Copyright: © 2021 by the authors. Licensee MDPI, Basel, Switzerland. This article is an open access article distributed under the terms and conditions of the Creative Commons Attribution (CC BY) license (<https://creativecommons.org/licenses/by/4.0/>).

1. Introduction

Colorectal cancer (CRC), one of the most serious health issues globally, ranks third in incidence and second in mortality among cancers worldwide. Chemotherapy, a baseline treatment for colorectal cancer, should be limited in the clinics due to the high resistance of cancer cells and the number of side effects. More than 1.8 million new cases were diagnosed in 2018, and approximately 20% of new CRC cases were confirmed as metastatic [1]. The phrase 'more is less' should be treated as a cornerstone of future efforts regarding establishing novel CRC clinical protocols, in which combining 'classical chemotherapy' with targeted therapy would improve the survival of patients with minimal side effects. The study evaluating some novel combinations of active agents can point the appealing and tempting pathways for future clinical efforts.

The regular use of nonsteroidal anti-inflammatory drugs (NSAIDs) is believed to trigger a prominent anticancer effect, as the increased level of prostaglandins within CRC tissue was detected [2,3]. The possibility of NSAID use in colon cancer prevention has been supported by growing evidence from several observational studies and post-trial follow-up data. Aspirin (ASA) and indomethacin were proven to be the most effective at reducing CRC risk amongst all cancers [2–4]. The comprehensive meta-analysis by Bosetti et al., supported earlier conclusions and confirmed an inverse association between regular ASA use and the risk of CRC and other digestive tract cancers [4]. ASA's anti-tumor activity is believed to be based on a selective induction of apoptosis in cancer cells [5,6]. However, the mechanism underlying its pro-apoptotic activity is complex and remains elusive.

Most of the ASA experiments and clinical trials were carried out to analyze its preventive role in tumorigenesis, while therapeutic effects have rarely been mentioned. Several

clinical trials assess whether ASA can increase disease-free survival in cancer patients (trial identifiers: NCT02467582; NCT02301286; NCT02945033; NCT03170115 at clinicaltrials.gov). Numerous results evidenced that the final therapeutic efficacy of ASA depends on the other chemotherapeutic drug applied in combination with this compound. The observation that ASA presented synergistic activity with anti-PD-L1 antibody (Ab) in the treatment of human tumors [7] laid the foundation for a clinical trial of their combined use in ovarian cancer patients (NCT02659384).

Fas (Fas, also known as CD95 molecule), a member of the tumor necrosis factor (TNF) receptor family, has been extensively studied for its proapoptotic function [8,9]. Fas receptor, Fas-mediated apoptotic pathway can be triggered by the caspase cascade activation, including a caspase-3 (one of the effector caspases). However, Fas signaling was also associated with non-apoptotic activities in cancer cells [10–15]. It was experimentally estimated that the level of Fas in cancer cell membranes necessary for their survival is 1000 times lower than the level required for its pro-apoptotic signaling [11]. Fas-mediated non-apoptotic activity is involved in a variety of signaling pathways independent of the death-promoting track [11,14,16–19]. The mechanisms regulating whether Fas triggers pro- or non-apoptotic signals remain to be fully explained.

The preliminary assumption is that ASA and anti-Fas antibody (Ab) exert synergistic effect targeting cancer stem cells (CSCs) derived from human CRC cell lines. However, the final effect depends on the cancer cell line used for the analysis [20]. The current manuscript presents the results of experiments evaluating this original hypothesis. The literature and our previous data motivated us to thoroughly analyze Fas signaling functions in CRC progression [20]. The detailed role of Fas signaling for CSCs features and viability are still not fully evident. Since the CSCs vulnerability to Fas ligand (FasL) was demonstrated by the Marcus Peter group [21], the issues of harnessing Fas to CSC elimination is appealing.

Our study aims to present the potential therapeutic activity of ASA administrated simultaneously with anti-Fas Ab in CRC cell lines. The comprehensive analysis of various effects, including CRC cells phenotype change, spherogenicity or cellular viability, that can be associated with treatment effectiveness, was conducted.

2. Materials and Methods

2.1. Expansion of HCT116 and HT29 Cell Lines and Incubation with Active Compounds

The HT29 and HCT116 cell lines (obtained originally from the American Type Culture Collection (ATCC, Manassas, VA, USA) were utilized in this study. HT29 cells origin from rectosigmoid part of intestine, whereas HCT116 is adenocarcinoma cells line, however, for simplicity of our manuscript, the cells analyzed from both cell lines we defined as colorectal cancer stem cells. These cells were cultured routinely as a monolayer in McCoy's medium, supplemented with 10% fetal bovine serum (FBS), 1% penicillin-streptomycin and 2 mL-glutamine and incubated at 37°C under a humidified atmosphere of 5% CO₂. The cells were serially subcultured by trypsin treatment when they achieved 80% confluence, and the medium was renewed 2–3 times/week.

For the current study, HCT116 and HT29 cell lines were cultured in spheroid forms (colonospheres, tumorspheres) that were grown in stem cell medium (SCM) established previously by our group [20,22,23]. In brief, cells were maintained in serum-free DMEM-F12 medium supplemented with ITS Liquid Media Complement (1×), bovine serum albumin (BSA, 4 mg/mL), glucose (3 mL/mL), Hepes (5 mM), L-glutamine (2 nM), heparin (4 µg/mL), EGF (20 ng/mL), bFGF (20 ng/mL), and antibiotic antimycotic solution (1×). All culture supplements and media were obtained from Sigma–Merck.

8×10^5 cells were seeded in 24-well ultra-low attachment plates and maintained in SCM. After three passages, newly formed spheres were treated with: acetylsalicylic acid (ASA) (Sigma-Aldrich, Poznan, Poland) at following concentrations: 2.2 mM, for HCT116 cells or 1.8 mM, for HT29 cells; anti-Fas (BD, IgM, clone EOS9.1) at the concentration 200 ng/mL (or concomitant control antibodies from Thermo Fisher Scientific) or their combinations dissolved in a freshly prepared culture medium. Additionally, for some

stimulations, 50 μM 5-fluorouracil (5-FU) (Sigma-Aldrich) (the most commonly used agent for CRC chemotherapeutic protocols) was used. 5-FU solution was prepared in DMEM/F12 medium, whereas ASA was dissolved in dimethyl sulphoxide (DMSO). In all experiments, the DMSO concentration was never higher than 1% (*v/v*) and did not affect cell growth (according to our initial study). All solutions were prepared immediately before use. The control cells were maintained in the SCM. The medium was replaced every 2–3 days to keep antibody and ASA concentration at an equally high level. After 10 days, the cell cultures were analyzed.

2.2. Generation and Expansion of DCs from Peripheral Blood Monocytes of Healthy Donors

We used leukocyte-platelet buffy coats ($n = 6$) obtained from volunteers recruited during routine medical consultations in the Regional Blood Bank in Gdansk, Poland, and only healthy individuals were included in this study. Peripheral blood mononuclear cells were separated by Histopaque[®]-1077 gradient centrifugation at 1200 g, 30 min at room temperature (RT). After isolation and erythrocytes' lysis, cells were washed and prepared for further isolation steps. To separate monocytes, PBMCs were cultured for 24 h on an adhesive Petri dish in RPMI 1640 supplemented with FBS (10%), L-glutamine (2 mM), penicillin (100 U/mL) and streptomycin (100 $\mu\text{g}/\text{mL}$), at 37 °C, 5% CO₂, 95% humidity. After incubation, a medium containing non-adherent cells was gently removed, and the plate with adherent cells was put on ice for 30 min. Afterwards, the monocyte layer was harvested using a scraper.

A total of 1×10^6 adherent cells (comprising mostly monocytes, as confirmed by flow cytometry)/1 mL were placed on 24-well plates in a medium supplemented with GM-CSF (50 ng/mL) and IL-4 (100 ng/mL) for 7 days. On day 3, half of the medium was replaced with a fresh medium containing these cytokines. On day 6, cells were subjected to maturation for 24 h in the presence of LPS (50 $\mu\text{g}/\text{mL}$) or cancer cell lysates. Lysates were obtained from the culture of HCT116 and HT29 cell lines (allogenic in relation to DCs). Untreated DCs (immature, iDCs) were regarded as control.

Cells' differentiation and maturation were monitored and documented using Olympus CKX53 inverted microscope coupled with digital camera Olympus SC50 (Olympus, Japan). The analysis and measurements of DCs length were performed using Olympus cellSens software (Olympus, Japan).

2.3. Flow Cytometric Analysis of Cell Phenotype

CRC cell lines and dendritic cells were stained with the following cocktail of monoclonal antibodies purchased from BD Biosciences, USA: anti-CD29-APC (clone MAR4, IgG1 κ), anti-CD44-FITC (clone C26, IgG2b κ), anti-CD95-PE (clone DX2, C3H/Bi IgG1 κ), anti-FasL Biotin (clone NOK-1, IgG1) coupled with Streptavidin-APC, anti-CD11c-APC (clone S-HCL-3, IgG2b), anti-CD80-PE (clone L307, IgG1 κ), anti-CD83-APC (clone HB15e, IgG1 κ), anti-HLA-DR-PerCP (clone L243, IgG2a). Anti-CD133/2-PE (clone 293C3, IgG2b κ) monoclonal antibodies were purchased from Miltenyi Biotec. After 30 min of incubation in the dark, samples were fixed with PBS containing 1 mM EDTA and prepared for further analyses. Flow cytometric analyses were performed using FACS Calibur flow cytometer (BD Biosciences, Franklin Lakes, NJ, USA) with BD CellQuest Pro software. During the analysis the dead cells and debris were excluded on SSC/FSC dot plot. Next, populations expressing particular specific surface markers were distinguished and measured. Unstained cells were used to set a threshold of positive signal. Data are presented as mean fluorescent intensity (MFI) related to unstained control MFI value.

2.4. Analysis of Apoptosis

According to the manufacturer's instructions, levels of CRC cell apoptosis were measured using an Annexin V-FITC Apoptosis Detection Kit[™] (BD Biosciences, Franklin Lakes, NJ, USA). Briefly, 5×10^5 spherical HCT116 and HT29 CRC cells were suspended in a staining mixture comprised of 100 μL binding buffer, 5 μL Annexin V-FITC and 5 μL pro-

pidium iodide. After 15 min incubation in RT in the dark, samples were diluted in Binding Buffer and prepared for further analysis. Flow cytometric analyses were performed within 30 min using FACS Calibur flow cytometer (BD Biosciences, Franklin Lakes, NJ, USA).

2.5. Quantification of Sphere Sizes

We measured the diameter of the spheres obtained from HCT116 and HT29 cells cultured in sphere-forming media for 10 days of continuous treatment. The analysis was conducted with the use of an inverted microscope Olympus-CKX53 coupled with a digital camera Olympus SC50. At least 50 spheres of each experimental option were measured.

2.6. CRC Cell Lines–Derived Lysates Preparation for the In Vitro Modification of DCs

HCT116 and HT29 cells were pooled, counted and afterwards used for the lysate preparation. Lysates were obtained by 4 repeating freeze-thaw cycles (by the sequential keeping vials with cells at $-80\text{ }^{\circ}\text{C}$ and $+36\text{ }^{\circ}\text{C}$) followed by filtration through $0.2\text{ }\mu\text{m}$ strainer. DCs were stimulated with lysates and the proportion between the number of cancer cells taken for lysates' preparation and DCs was 1:1. For this goal, CRC cells were treated with ASA (at concentrations given above) and anti-Fas Ab, and additionally with $50\text{ }\mu\text{M}$ 5-fluorouracil (5-FU) (Sigma-Aldrich).

2.7. Western Blot Analysis of Caspase-2 and Caspase-3

Cell lysates were prepared by 4 repeated freeze-thaw cycles, as described above. Protein concentration in the lysates was measured with Bradford reagent (Sigma-Aldrich). Protein samples ($10\text{ }\mu\text{g}$) were loaded to 4–20% Mini-PROTEAN[®] TGX[™] Precast Protein Gels (Bio-Rad, Warszawa, Poland) and transferred to a PVDF membrane using the Trans-Blot Turbo system (Bio-Rad). Membranes were blocked with 5% non-fat milk in TBS buffer with 0.1% Tween 20 (TBST) for 1 h at RT. Incubation with rabbit monoclonal anti-caspase-2 antibody (1:500; Abcam) and rabbit monoclonal anti-caspase-3 antibody (1:1000; Abcam) was performed overnight at $4\text{ }^{\circ}\text{C}$. After triple washing with TBST, blots were incubated for 1.5 h at RT with horseradish peroxidase-conjugated anti-rabbit IgG antibody (1:10,000; Sigma-Aldrich). Anti-GAPDH peroxidase-conjugated IgM antibody (1:50,000, 1 h RT; Sigma-Aldrich) was used for the loading control. According to the manufacturer's protocol, visualization was performed using chemiluminescence enhanced with a luminol reagent (Bio-Rad). The signal was read using ImageQuant LAS 500 (GE Healthcare, Warszawa, Poland). Densitometric analysis of immunoreactive protein bands was performed with Quantity One software (Bio-Rad) and calculated as Units = Intensity/ mm^2 normalized to GAPDH protein units content in each sample. Each experiment was performed in triplicate, except HCT116 caspase-2 analysis which was performed in duplicate. Proteins assessed by western blot had molecular weights 51 kDa, 37 kDa and 38 kDa for caspase-2, caspase-3 and GAPDH, respectively.

2.8. Statistical Analysis

All data obtained during the study were analyzed using GraphPad Prism v. 6.05 (GraphPad Software, San Diego, CA, USA) according to the non-parametric U Mann-Whitney test or Kruskal-Wallis test followed by Dunn's test as a post hoc procedure. Values of $p < 0.05$ were considered as statistically significant. Data in figures are presented as median \pm interquartile range or median with min-max values.

3. Results

3.1. ASA and Anti-Fas Ab Influenced the Diameter of HCT116 and HT29–Derived Colonospheres

Cancer cells of two human CRC lines were treated with the combination of anti-Fas agonistic antibody (200 ng/mL) and 2.2 mM and 1.8 mM ASA for HCT116 and HT29 cell lines, respectively. After 10 days of treatment colonospheres sizes, phenotype and apoptosis were measured.

In order to establish the proper working concentrations of ASA in our cell lines, we determined the IC₅₀ of ASA using a cytotoxicity assay after 24 h-incubation and ASA concentrations based on the previously published results [24–26]. Our analysis shown an IC₅₀ 2.2 mM and 1.8 mM of ASA for HCT116 and HT29, respectively. The concentration of anti-Fas antibody (200 ng/mL) was evaluated in our previous study [20].

Following the combined stimulation with anti-Fas Ab and ASA spheres were statistically significantly smaller compared to the size of spheres after incubation with ASA only and control, untreated colonospheres (Figures 1 and 2). Similarly, colonospheres after stimulation with anti-Fas Ab were relevantly bigger than those after combined treatment, and these differences were statistically significant. This observation confirmed our previous results showing that Fas signaling may play a pro-survival role for cancer cells [20].

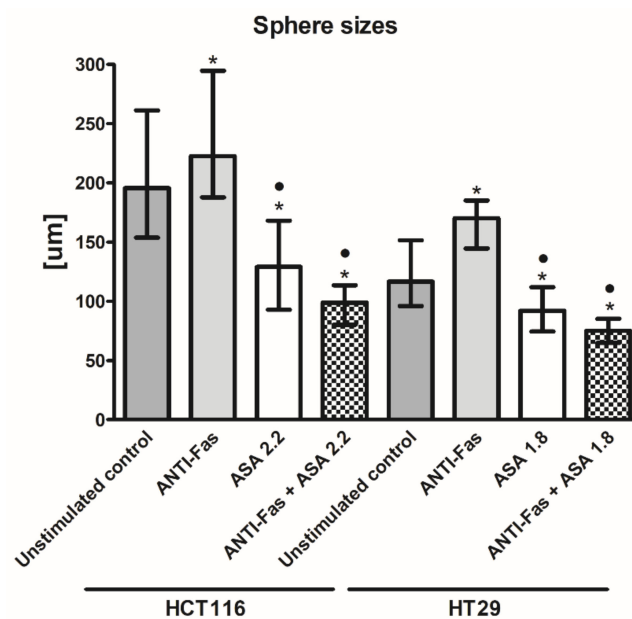


Figure 1. Sizes of colonospheres. Colonospheres were formed from HCT116 or HT29 cells following 10-day incubation with agonistic anti-Fas antibody (200 ng/mL) and/or aspirin (ASA) (2.2 mM or 1.8 mM for HCT116 or HT29, respectively). Statistically significant differences were assessed by Kruskal-Wallis test followed by Dunn's test as a post hoc procedure. Bars and whiskers represent median \pm interquartile range (* $p < 0.05$ vs control unstimulated cells, • $p < 0.05$ ASA vs ASA/anti-Fas antibody, $n = 50$ –60).

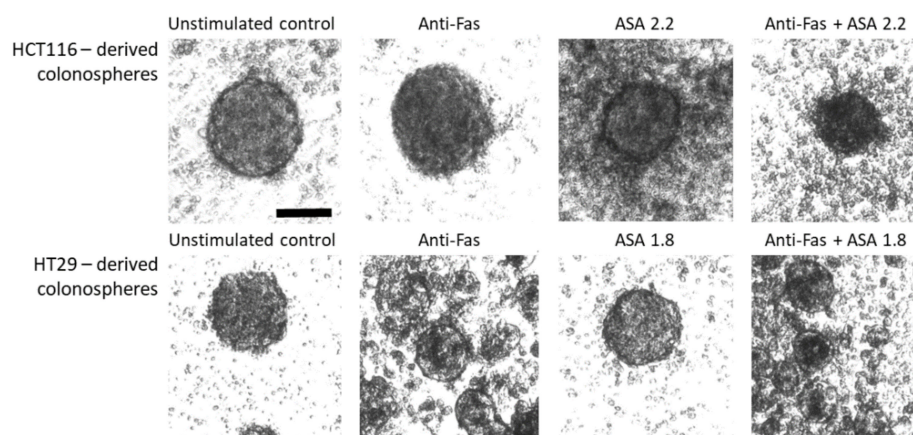


Figure 2. Morphology of colonospheres. Representative colonospheres were derived from HCT116 and HT29 cells following 10-day incubation with agonistic anti-Fas antibody (200 ng/mL) and/or aspirin (ASA) (2.2 mM or 1.8 mM for HCT116 or HT29, respectively). Scale bar, 100 μ m.

3.2. ASA and Anti-Fas Ab Impact on the Phenotype of Hct116 and Ht29–Derived Colonospheres

Cells of CRC lines cultured in the form of colonospheres and treated for 10 days with ASA and/or anti-Fas Ab were subjected to cytometric analysis of commonly used stem cell surface markers. We have previously presented that HT29 and HCT116 cell lines cultured in spherical form are highly heterogeneous and enriched in cells bearing some CSC-like features [20,23]. Multicellular spheroid model of cancer cells' expansion seems to partially simulate naturally-occurring heterogeneity in regard to cellular morphology, heterogeneous exposure to environmental factors and specific gene expression [27,28]. Since the CSCs are the most important clinical challenge we decided to focus our attempts on this critical cancer cells' population. In the current study we could observe that the influence of treatment on colonosphere cells depended on the cancer cell line used (Figure 3).

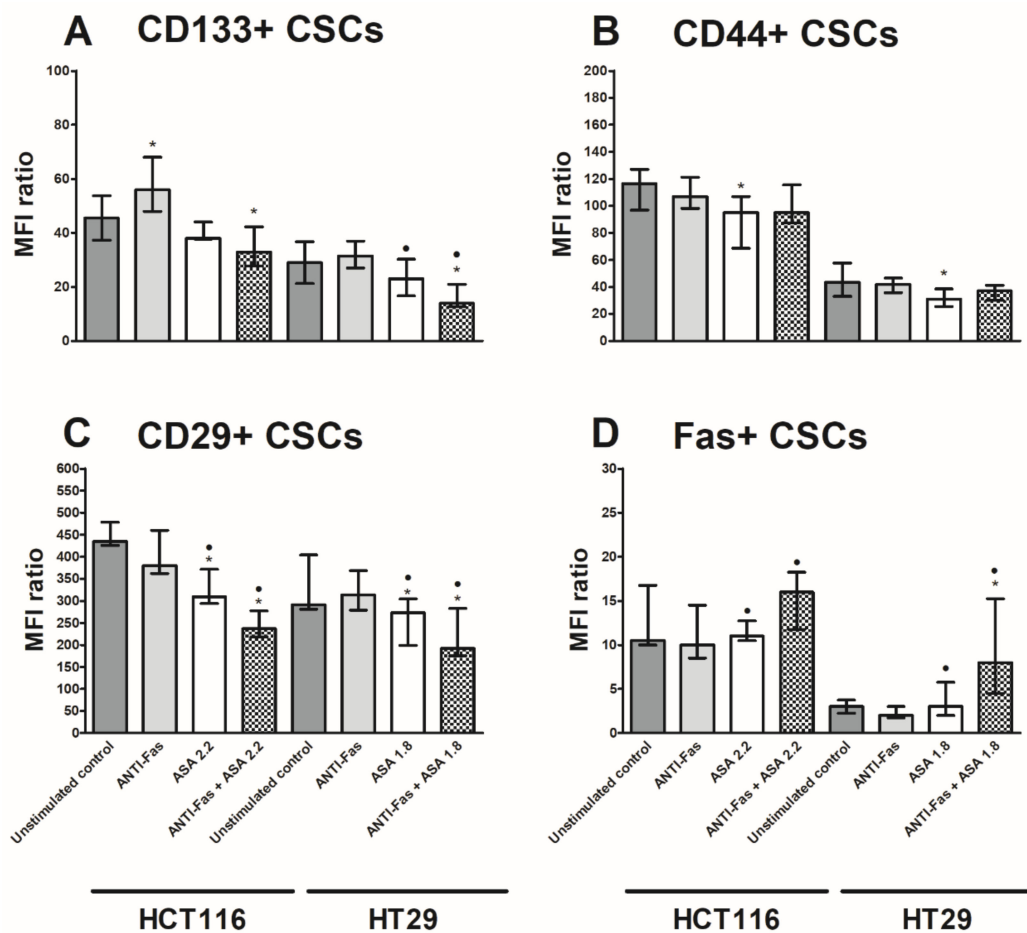


Figure 3. The cytometric analysis of HCT116 and HT29 cells expanded 10 days in spherical forms with agonistic anti-Fas antibody (200 ng/mL) and/or aspirin (ASA) (2.2 mM or 1.8 mM for HCT116 or HT29, respectively). Y-axis presents mean fluorescence intensity (MFI) related to unstained control. Statistically significant differences were assessed by Kruskal-Wallis test followed by Dunn's test as a post hoc procedure or U Mann-Whitney test. Bars and whiskers represent median \pm interquartile range (* $p < 0.05$ vs control unstimulated cells, • $p < 0.05$ ASA vs ASA/anti-Fas antibody, $n = 12$ for each option). Triplicate independent experiments were performed. (A–D). The analysis of CD133⁺, CD44⁺, CD29⁺ and Fas⁺ colorectal cancer stem cells (CSCs), respectively.

Our results revealed that the percentage of CD133⁺, CD44⁺ and CD29⁺ cells in both CRC cell lines presented the same pattern of changes. We could observe that ASA reduced the number of CSCs bearing particular markers and ASA combined with anti-Fas Ab-intensified this phenomenon (Figure 3A–C). The most significant differences were observed for MFI values of CD29 protein. CD133⁺ cells number significantly decreased after the combined treatment (Figure 3A), and this turned out to depend on ASA concentration

(data not shown). Subsequently, we checked cytometrically how the introduced treatment influenced CD133+ Fas+ (CD95+) cell number among both cancer cell lines (Figure 3D). HCT116 and HT29 cells reacted in similar way with significant elevation of MFI values after simultaneous treatment with ASA and anti-Fas Ab.

3.3. The Analysis of HCT116 and HT29 Cell Death after Their Treatment with ASA and Anti-Fas Ab

Since the Fas signaling in its canonical form is pro-apoptotic, we decided to correlate the dying/apoptosis rate with all previously presented parameters. The proportion of apoptotic cells was assessed using flow cytometry and Annexin V-FITC and PI staining. Despite the elevated percentage of nonviable cells found in colonospheres, the overall number of cells within these structures was constant and as we stated in our previous manuscript, it was the result of cell differentiation and weaker cell-cell interactions [23]. The cell death was quantified after 10 days of cells' incubation with ASA and/or anti-Fas Ab. Additional isotype control IgM Ab wasn't found to influence the viability of cells following the introduced treatment. We found that the isotype control IgM Ab exerted no statistically significant impact also on cells phenotype in our experimental conditions (data not shown).

Our analyses revealed that combined treatment induced more intensive apoptosis of CSCs in our culture conditions (Figure 4). The treatment of HCT116 and HT29 cells with anti-Fas Ab and ASA induced a higher rate of apoptosis than the effect observed in cultures of untreated cells or treated exclusively with anti-Fas Ab. The number of apoptotic cells was consistent with the level of caspase-3 measured in our samples by Western blot (Figure 5).

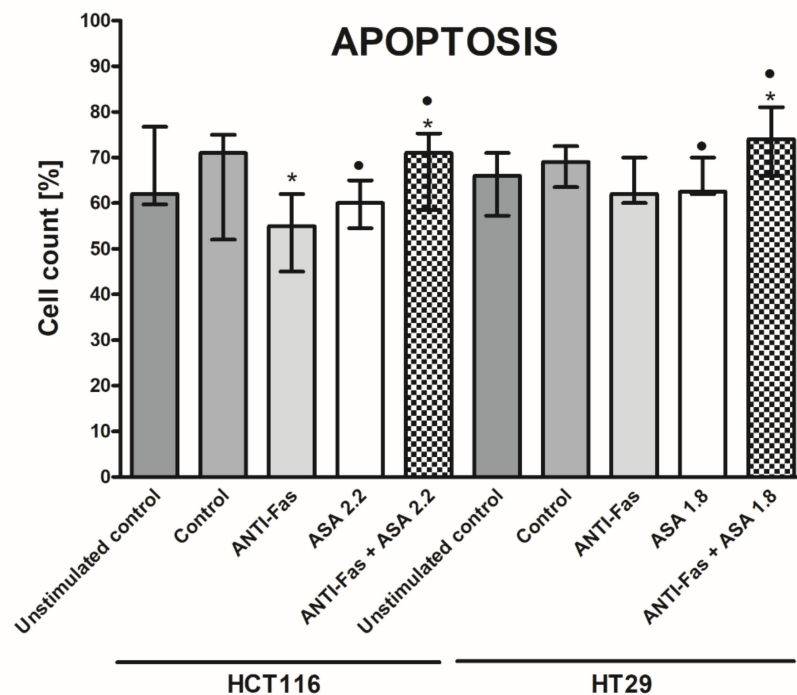


Figure 4. The cytometric analysis of cells' apoptosis during 10 day–expansion of HCT116 and HT29 cells in spherical forms with agonistic anti-Fas antibody (200 ng/mL), isotype control IgM Ab and/or aspirin (ASA) (2.2 mM or 1.8 mM for HCT116 or HT29, respectively). Annexin V–FITC/PI were used for assessing apoptotic cells. Y-axis presents Annexin V + PI cells frequency (%). Statistically significant differences were assessed by Kruskal–Wallis test followed by Dunn's test as a post hoc procedure. Bars and whiskers represent median \pm interquartile range (* $p < 0.05$ vs control unstimulated cells, • $p < 0.05$ ASA vs ASA/anti-Fas antibody, $n = 12$ for each option). Triplicate independent experiments were performed.

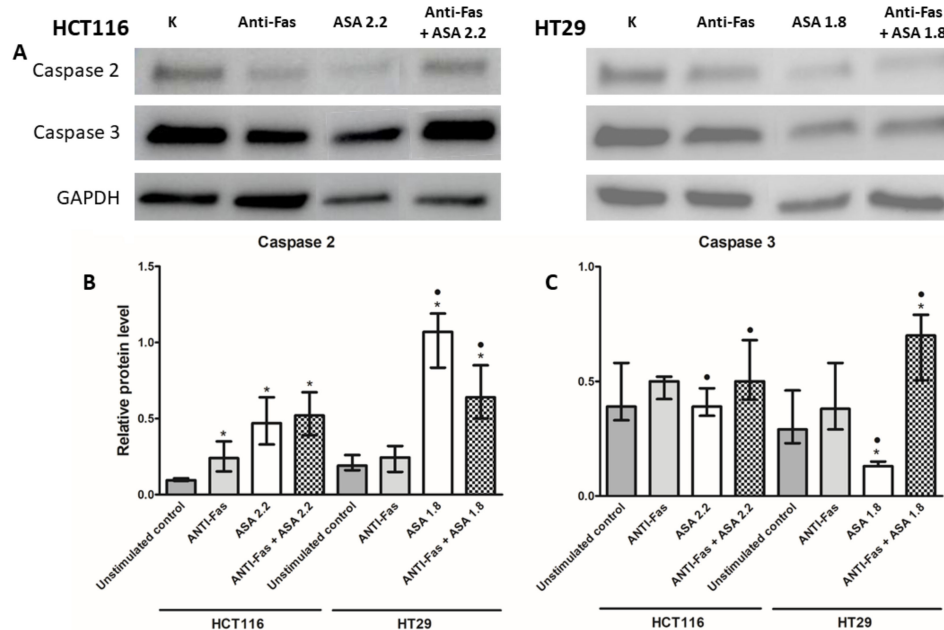


Figure 5. (A) Representative western blot analysis images of caspase-2 and caspase-3 proteins in HCT116 and HT29 cells expanded 10 days in spherical forms with agonistic anti-Fas antibody (200 ng/mL) and/or aspirin (ASA) (2.2 mM or 1.8 mM for HCT116 or HT29, respectively). Protein assessment was performed as described in the Materials and methods. Merged image of all proteins as they were analyzed in the same western blot membrane. (B,C). Densitometric analysis of the caspase-2 (B) and caspase-3 (C) expression at the protein level by western blot. Bars and whiskers represent median \pm interquartile range normalized to GAPDH level in each sample (* $p < 0.05$ vs. control unstimulated cells, • $p < 0.05$ ASA vs. ASA/anti-Fas antibody). Statistically significant differences were assessed by Kruskal-Wallis test followed by Dunn's test as a post hoc procedure. Each experiment was performed in triplicate, except HCT116 caspase-2 analysis which was performed in duplicate.

Since caspases are the essential proteins engaged in diverse death pathways, in the next step of our study, we evaluated the protein level of caspase-2 and caspase-3 with Western blot (Figure 5). Our results demonstrated the variability of caspase-2 relative level. HCT116 spheroids were found to express the highest caspase-2 after combined treatment, while HT29 cells presented the highest content of this protein following incubation only with ASA. These differences were statistically significant in comparison to control, untreated cells. Moreover, we discovered that combined treatment resulted in increased levels of caspase-3 in both cell lines (Figure 5) ($p < 0.05$, U Mann-Whitney test).

Surprisingly, the elevated level of caspase-3 was observed in the same HCT116 cells, which displayed also elevated caspase-2 (after ASA + anti-Fas Ab incubation) (Figure 5). At the same time HT29 cancer cells presented inverted tendency in caspases expression. The differences visible in the effect induced in HCT116 and HT29 CRC cell lines are probably associated with different cancer progression status (HCT116–TNM3, HT29–TNM2) and distinct gene status of these cells (e.g., KRAS: G13D and WT; BRAF: WT and V600E; PIK3CA: H1047R and P449T; PTEN: WT and WT; TP53: WT and R273H for HCT116 and HT29 cell line, respectively) [29].

3.4. Influence of ASA and/or Anti-Fas Ab Treatment on DCs Length

We assume that the simultaneous colonospheres' treatment with ASA and anti-Fas Ab exerted an advantageous effect against CRC cells. Our group has recently analyzed dendritic cells in anti-cancerous context [22]; thus we decided to test whether our experimental conditions used for the treatment of CRC CSCs would have a significant impact on DCs basic features after their in vitro modification. We have previously shown that cancer cells-derived lysates and conditioned medium can improve the efficacy of DCs preparation for potential DC-based immunotherapy, especially when administrated with LPS [22].

The current study design included DC incubation with lysates obtained from HCT116 and HT29 CRC cells treated with ASA and/or anti-Fas Ab. DCs are known to navigate anti-cancerous response, especially during the first, initial phases of cancer progression [30] thus the analysis of their reaction seems to be reasonable.

Colonspheres after 10-day incubation with anti-Fas Ab and/or ASA, or 5-FU were polled and cellular lysates were prepared according to commonly used method relying on freezing and thawing sequences as described previously [22]. Afterwards, DCs obtained from monocytes of healthy volunteers were stimulated for 24 h with 100 μ L of lysates of colorectal cancer cells or with LPS. LPS, a potent DC activator, was used as the specific internal positive control of stimulatory potential. We assessed the morphological diversity of obtained DCs with a digital camera and measured DCs length to estimate the particular lysates influence (Figure 6). The DC length analysis revealed that the final effect depended on the cell line used for lysates preparation. HCT116-derived lysates exerted a more prominent impact on DCs size in comparison to HT29-derived lysates. For HT29-derived lysates, we noticed a less dynamic effect since the incubation of DC with lysates didn't change the DCs length. For almost all of our experimental options, the size of DCs was significantly smaller than size of DCs stimulated with LPS. The incubation of DCs with lysates of HCT116 and HT29 cells pretreated with 5-FU resulted in shortening of DCs and these cells were smaller than DCs after ASA/anti-Fas stimulation. Comparing the effect of lysates obtained after stimulation of CRC cell lines with ASA \pm anti-Fas Ab, we observed opposite results for the studied cell lines. Additionally, HCT116 cells stimulated with both ASA and anti-Fas Ab provided lysates which increased the size of DCs more effectively than ASA-stimulated CRC cells.

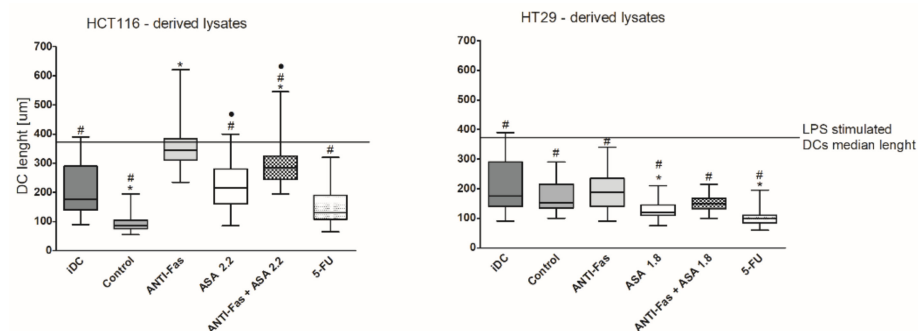


Figure 6. The length [μ m] of DCs expanded from monocytes and incubated for 24 h with LPS or lysates of HCT116 and HT29 cells expanded for 10 days in spherical forms with agonistic anti-Fas antibody (200 ng/mL) and/or aspirin ASA (2.2 mM or 1.8 mM for HCT116 or HT29, respectively), or 5-FU (50 μ M) in comparison to immature unstimulated DCs (iDCs). DCs incubated with lysates prepared from cancer cells not treated are defined as CONTROL in the Figure. Boxes and whiskers represent min-max, lines—median values. The LPS-stimulated median value of DCs' length was set on Y-axis. Statistically significant differences were assessed by Kruskal-Wallis test followed by Dunn's test as a post hoc procedure. (* $p < 0.05$ vs iDCs, • $p < 0.05$ ASA vs ASA/anti-Fas antibody, # $p < 0.05$ vs LPS, $n = 60$ –80 of each option). Three independent experiments were performed.

3.5. Influence of ASA and/or Anti-Fas Ab Treatment on DCs Phenotype

DCs were harvested and subjected to flow cytometry phenotypic analysis, which revealed that the number of CD11c+, HLA-DR+, CD80+ and CD83+ DCs was altered in a cell line dependent manner (Figure 7). Lysates derived from HCT116 cells pretreated with ASA and anti-Fas Ab induced more significant changes of DCs' proportions in comparison to HT29-derived lysates. Only the proportion of CD11c+ DCs extended over the level caused by LPS (Figure 7A,B). We could observe the relevantly increased proportion of activated DCs after incubation with lysates prepared with CRC cells incubated with ASA and/or anti-Fas Ab in comparison to control unstimulated cells (iDCs). There were some exceptions, for instance, anti-Fas Ab when used alone often kept the DCs status on the same level as iDCs (Figure 7B,D,E).

The effect of 5-FU-treated CRC cells on DCs was found very diverse, in some experimental options the proportion of DCs with studied markers was elevated (Figure 7A,C), in other cases—decreased after in vitro modification (Figure 7E,F,H) in comparison to iDCs.

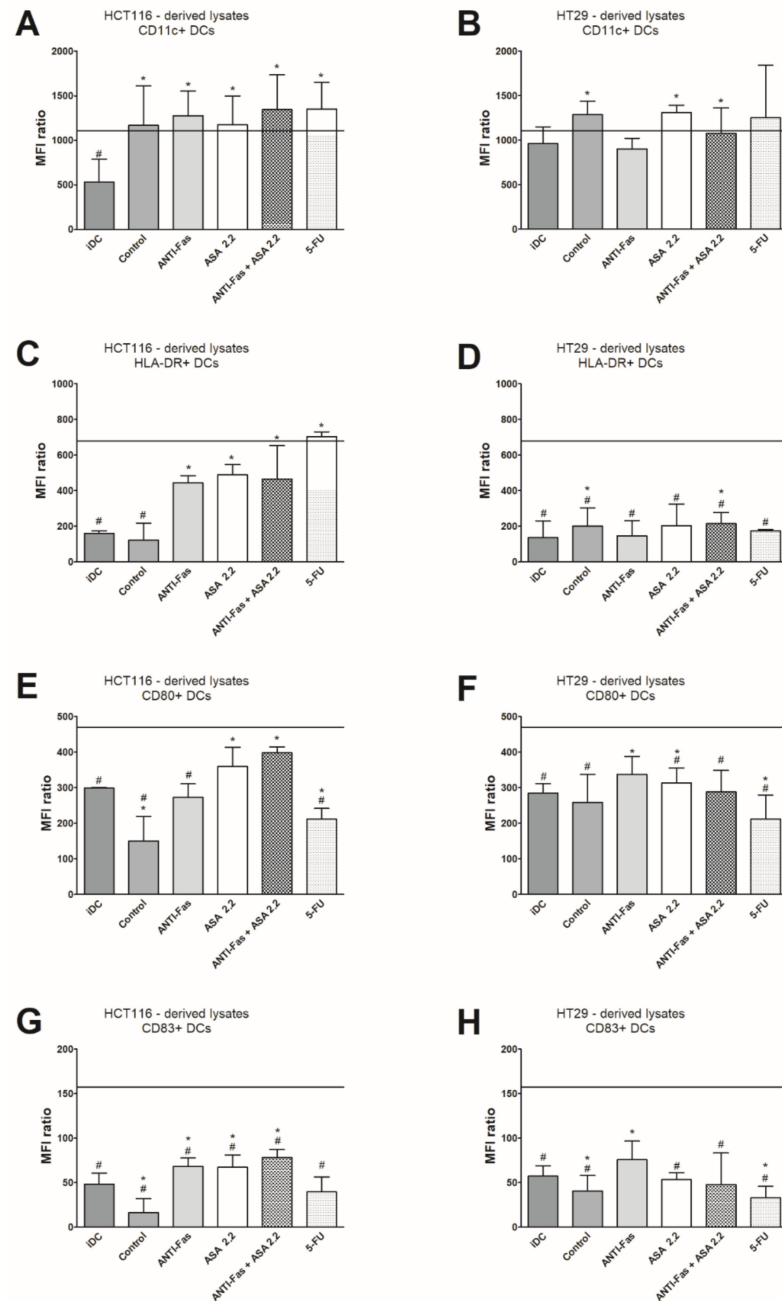


Figure 7. The effect of cancer cell lysates or LPS on the proportions of CD11c+ (A,B), HLA-DR+ (C,D), CD80+ (E,F) and CD83+ (G,H) DCs. Data are presented as mean fluorescence intensity (MFI) related to unstained control. Lysates used in these analyses were collected from cultures of HCT116 and HT29 CRC cell lines expanded for 10 days in spherical forms with agonistic anti-Fas antibody (200 ng/mL) and/or aspirin (ASA) (2.2 mM or 1.8 mM for HCT116 or HT29, respectively), or 5-FU (50 µM). The value of LPS–stimulated DCs was set on Y-axis with continuous line. DCs incubated with lysates prepared from cancer cells not treated are defined as CONTROL in the Figure. Bars and whiskers represent median ± interquartile range. Statistically significant differences assessed by Kruskal-Wallis test were followed by Dunn’s test as a post hoc procedure or U Mann-Whitney test. (* $p < 0.05$ vs iDCs, # $p < 0.05$ vs LPS). Three independent experiments were performed. M.

4. Discussion

Our initial analyses provided a surprising and interesting observation that ASA can modulate the impact of pro-cancerous Fas signaling on HCT116 and HT29 cancer cell lines. Our results suggested the synergistic relationship between both active compounds: ASA and anti-Fas Ab. Currently, the shortage of reports combining the activity of ASA and anti-Fas Ab is highlighted by the increasing number of data depicting these agents' independent activity in different contexts and conditions, including anti-cancer effect.

In our experimental panel, ASA when added alone for cancer cells' treatment, reduced sphere sizes but at the same time the number of CD133+ CSCs was the same as in control. Original pro-cancerous role of Fas signaling (previously presented in [20]) was ceased after ASA was included into samples. We found that simultaneous treatment induced the reduction of sphere sizes, the number of CD133+, CD44+ and CD29+ cancer cells in colonospheres, along with higher apoptosis rate. Incubation with ASA + anti-Fas Ab elevated the number of Fas+ cancer cells (probably more vulnerable to apoptosis) what is confirmed by cytometric apoptosis assay. Moreover, in samples with higher apoptosis, the higher caspase-2 and-3 protein relative levels were also found. Moreover, the level of caspases remains at higher level than in control. Our combined treatment modified the caspases level what seemed to influence other measured parameters. Our results highlighted the potential crucial role of caspases in CSCs function in both cancer cell lines we used.

To establish the type of cell death and/or pro-tumorigenic activity resulting from the combined treatment of CRC CSCs with anti-Fas Ab and ASA, we assessed the levels of caspase-2 and caspase-3, the latter known as an executioner type of a cysteine-aspartic protease involved in the apoptotic process. Recently Quadir et al., have shown that caspase-3 inhibitor didn't enhance STAT1 activation and the lack of caspase-3 expression resulted in the Fas signaling activation even without its stimulation [31].

Caspase-3 is known to be associated with stemness of CSCs and Flanagan et al., revealed that a subgroup of CRC patients with low levels of an active form of caspase-3 was characterized by increased disease-free survival [32]. Moreover, Huang et al., in in vitro and in vivo experiments proved that dying breast cancer cells following radiotherapy produced caspase-3 and other paracrine factors that stimulated the growth of the remaining cancer cell population [33]. Our observations seem to confirm these results. Although we measured the non-cleaved form of caspase-3, the elevated relative level of this protein was clearly visible in samples with the most advanced apoptosis. It is commonly believed that the active form of caspase-3 is directly engaged in apoptosis since not the whole pool of proteins after translation can be a trigger for the executioner phase of programmed cell death. Since we discovered a similar phenomenon in both studied CRC cell lines, the elevated caspase-3 level seems to have a biologically relevant meaning and require further analyzes. In these samples the low proportion of CD133+ cells is probably associated with the silencing of CSCs metabolism for cancer evasion, protecting mechanism from anti-cancerous agents.

It is well known that caspases may participate in different cell death types, i.e., apoptosis, necroptosis and DICE (death induced by CD95 or CD95L elimination) [31,34]. However, it has to be stressed that their function is not limited to the regulation of cell death mechanisms [35]. Caspase-2 plays multiple roles in normal cells, including DNA-damage-induced apoptosis, cell cycle regulation and genomic stability maintenance. Moreover, cumulative evidence also implicates caspase-2 as an important driver of cell maturation and differentiation [34]. Caspase-2 was suggested to be a negative regulator of the Fas/STAT1 axis supporting stemness of cancer cells, demonstrated on the MCF-7 breast cancer cell line [31]. Moreover, a reduced level of caspase-2 was noticed upon Fas stimulation [31] and we also presented that treatment of CRC cells only with anti-Fas Ab did not exert a prominent effect on the caspase-2 level. In the same samples we found significantly elevated CD133+ CSCs count. At the same time, simultaneous stimulation of CRC cells with ASA and anti-Fas Ab

significantly (2–5 times) increased caspase-2 level in both studied cell lines with parallel lowering of CSCs proportion.

Based on previous observations that caspase-2 is not involved in the anti-apoptotic and pre-cancerous functions of Fas signaling [31], we hypothesized that this protein might antagonize the Fas pathway by being the natural inhibitor driving the elimination of CRC cells. Additionally, CSCs seem to be specific targets of such stimulation. Moreover, caspase-2 was described as an agent that triggers DICE, a necrotic form of mitotic catastrophe characterized by cell swelling, ROS production causing DNA damage and mitochondrial outer membrane permeabilization [31,36]. DICE was suggested to be the last resort allowing the specific elimination of cells lacking Fas and/or FasL.

We included into our study DCs to assess if lysates prepared from cancer cells treated with both active compounds would influence their activity. The analysis of DCs' phenotype seems to confirm that pretreatment of cancer cells before their engagement into in vitro modification of DCs can be beneficial for the final effect. We found that the lysates obtained from HCT116 colorectal cancer cells treated with our active compounds led to significantly enhanced expression of CD80 and CD83 markers on DCs surface, commonly associated with activation status of these cells. HT29-derived lysates exerted a less prominent effect on DCs what is probably associated with diverse cancer progression status of both CRC cell lines (HCT116–TNM3, HT29–TNM2). Nonetheless, this issue is open for further investigation since many different aspects of DC features and functions should be taken into consideration. Moreover, many previous results proved the influence of caspases in cancer milieu on the activity of immune cells, including DCs. Additionally, it has recently been suggested that mutations in caspase-3 might increase tumor recurrence risk after T cell-based cancer immunotherapy [37]. Previously, it was found that the number of mature CD11c+ MHCII+ DCs was significantly lower in caspase 3 gene knockout mice in comparison to wild type. The Authors suggested that caspase 3 may be involved in the regulation of maturation and anti-cancerous activity of DCs [38]. Moreover, it was demonstrated that DC and cytokine-induced killer cells significantly enhanced the apoptosis ratio of cancer stem cells of human hepatocellular carcinoma by, among others, increasing caspase-3 protein expression [39].

As we previously reported, anti-Fas stimulation has rather pro-cancerous effect since we found increased number of CD133+ and CD29+ CSCs, an increased sphere sizes, decreased apoptosis rate and most of these differences were significant comparing to untreated control cells [20] and the effect of anti-Fas treatment depended on the cell line used. The increased level of caspase-2 confirmed the association of Fas signaling with DICE (a necrotic form of mitotic catastrophe) which is believed to be characteristic for CSC population. Mentioned above pro-tumorigenic activity may be ceased by ASA, what was confirmed in the presented study by the increased apoptosis mediated by elevated caspase-3. Additionally, we noticed a decrease of CD133+, CD44+ and CD29+ CSCs in the total population of cancer cell lines. The increased number of CD44+ CD29+ cells among both CD133- and CD133+ populations (data not shown) is suggested to be associated with increased adhesive properties of remaining cells and was responsible for maintaining colonospheres' integrity.

The results provided by experiments on HCC (hepatocellular carcinoma) and sorafenib [40], lung cancer and methotrexate (MTX, an antimetabolite of the antifolate type) [41] and lung cancer CL1-0 and A549 cell lines and thiazolidinedione troglitazone (TGZ, oral anti-type II diabetes drug) [41] seem to confirm ASA's potential therapeutic activity depending on the cancer cell line used and the chemotherapeutic drug applied in combination with ASA. Additionally, some of these results suggested the cooperation between Fas and ASA. Fas signaling was demonstrated to support cancer development and expansion of CSCs [20,21]; thus, the approach which could counteract this unfavorable activity is needed. Although our research presents insights into ASA's effect on this phenomenon, there is still much to be elucidated.

Based on our results we assume that the fragile balance between caspase-2 and caspase-3 activity might be a key for the induction of either pro-stemness or anti-cancerous effects. ASA seems to influence this intracellular balance acting as the specific switch between different faces of Fas signaling. Summarizing, in this study, we have reported a previously unexplored combination of ASA and anti-Fas Ab to assess these biologically active compounds in vitro synergistic properties against colorectal cancer cell lines. This original concept need further analysis to unveil its real significance in cancer cell biology.

Author Contributions: Conceptualization, M.S.; methodology, M.S. and A.O.-K.; software, M.S. and A.W.; validation, M.S., A.O.-K. and A.W.; formal analysis, M.S. and A.W.; investigation, M.S., A.O.-K. and A.Z.; resources, M.S.; data curation, M.S.; writing—original draft preparation, M.S., A.O.-K. and A.W.; writing—review and editing, M.S. and Z.K.; visualization, M.S. and A.W.; supervision, M.S.; project administration, M.S.; funding acquisition, M.S. and Z.K. All authors have read and agreed to the published version of the manuscript.

Funding: The publication of this research manuscript was financed by the statutory grant (ST-12) of the Medical University of Gdansk, Poland.

Institutional Review Board Statement: Not applicable.

Informed Consent Statement: Not applicable.

Data Availability Statement: The datasets generated during and/or analyzed during the current study are available from the corresponding author on reasonable request.

Conflicts of Interest: The authors declare no conflict of interest.

References

1. Li, Z.-N.; Zhao, L.; Yu, L.-F.; Wei, M.-J. BRAF and KRAS mutations in metastatic colorectal cancer: Future perspectives for personalized therapy. *Gastroenterol. Rep.* **2020**, *8*, 192–205. [[CrossRef](#)]
2. Burn, J.; Sheth, H. The role of aspirin in preventing colorectal cancer. *Br. Med. Bull.* **2016**, *119*, 17–24. [[CrossRef](#)]
3. Nan, H.; Hutter, C.M.; Lin, Y.; Jacobs, E.J.; Ulrich, C.M.; White, E.; Baron, J.A.; Berndt, S.I.; Brenner, H.; Butterbach, K.; et al. Association of Aspirin and NSAID Use with Risk of Colorectal Cancer According to Genetic Variants. *JAMA* **2015**, *313*, 1133. [[CrossRef](#)] [[PubMed](#)]
4. Bosetti, C.; Santucci, C.; Gallus, S.; Martinetti, M.; La Vecchia, C. Aspirin and the risk of colorectal and other digestive tract cancers: An updated meta-analysis through 2019. *Ann. Oncol.* **2020**, *31*, 558–568. [[CrossRef](#)] [[PubMed](#)]
5. Qiu, W.; Wang, X.; Leibowitz, B.; Liu, H.; Barker, N.; Okada, H.; Oue, N.; Yasui, W.; Clevers, H.; Schoen, R.E.; et al. Chemoprevention by nonsteroidal anti-inflammatory drugs eliminates oncogenic intestinal stem cells via SMAC-dependent apoptosis. *Proc. Natl. Acad. Sci. USA* **2010**, *107*, 20027–20032. [[CrossRef](#)] [[PubMed](#)]
6. Piazza, G.A.; Rahm, A.K.; Finn, T.S.; Fryer, B.H.; Li, H.; Stoumen, A.L.; Pamukcu, R.; Ahnen, D.J. Apoptosis primarily accounts for the growth-inhibitory properties of sulindac metabolites and involves a mechanism that is independent of cyclooxygenase inhibition, cell cycle arrest, and p53 induction. *Cancer Res.* **1997**, *57*, 2452–2459.
7. Hamada, T.; Cao, Y.; Qian, Z.R.; Masugi, Y.; Nowak, J.A.; Yang, J.; Song, M.; Mima, K.; Kosumi, K.; Liu, L.; et al. Aspirin Use and Colorectal Cancer Survival According to Tumor CD274 (Programmed Cell Death 1 Ligand 1) Expression Status. *J. Clin. Oncol.* **2017**, *35*, 1836–1844. [[CrossRef](#)] [[PubMed](#)]
8. Le Gallo, M.; Poissonnier, A.; Blanco, P.; Legembre, P. CD95/Fas, Non-Apoptotic Signaling Pathways, and Kinases. *Front. Immunol.* **2017**, *8*, 1216. [[CrossRef](#)]
9. Levoine, N.; Jean, M.; Legembre, P. CD95 Structure, Aggregation and Cell Signaling. *Front. Cell Dev. Biol.* **2020**, *8*, 314. [[CrossRef](#)] [[PubMed](#)]
10. Martin-Villalba, A.; Llorens-Bobadilla, E.; Wollny, D. CD95 in cancer: Tool or target? *Trends Mol. Med.* **2013**, *19*, 329–335. [[CrossRef](#)]
11. Chen, L.; Park, S.-M.; Tumanov, A.V.; Hau, A.; Sawada, K.; Feig, C.; Turner, J.R.; Fu, Y.-X.; Romero, I.L.; Lengyel, E.; et al. CD95 promotes tumour growth. *Nature* **2010**, *465*, 492–496. [[CrossRef](#)]
12. Desbarats, J.; Newell, M.K. Fas engagement accelerates liver regeneration after partial hepatectomy. *Nat. Med.* **2000**, *6*, 920–923. [[CrossRef](#)]
13. Desbarats, J.; Birge, R.B.; Mimouni-Rongy, M.; Weinstein, D.E.; Palerme, J.-S.; Newell, M.K. Fas engagement induces neurite growth through ERK activation and p35 upregulation. *Nat. Cell Biol.* **2003**, *5*, 118–125. [[CrossRef](#)]
14. Zuliani, C.; Kleber, S.; Klussmann, S.; Wenger, T.; Kenzelmann, M.; Schreglmann, N.; Martinez, A.; del Rio, J.A.; Soriano, E.; Vodrazka, P.; et al. Control of neuronal branching by the death receptor CD95 (Fas/Apo-1). *Cell Death Differ.* **2006**, *13*, 31–40. [[CrossRef](#)]

15. Corsini, N.S.; Sancho-Martinez, I.; Laudenklos, S.; Glasgow, D.; Kumar, S.; Letellier, E.; Koch, P.; Teodorczyk, M.; Kleber, S.; Klussmann, S.; et al. The Death Receptor CD95 Activates Adult Neural Stem Cells for Working Memory Formation and Brain Repair. *Cell Stem Cell* **2009**, *5*, 178–190. [[CrossRef](#)] [[PubMed](#)]
16. Park, S.-M.; Schickel, R.; Peter, M.E. Nonapoptotic functions of FADD-binding death receptors and their signaling molecules. *Curr. Opin. Cell Biol.* **2005**, *17*, 610–616. [[CrossRef](#)]
17. Kleber, S.; Sancho-Martinez, I.; Wiestler, B.; Beisel, A.; Gieffers, C.; Hill, O.; Thiemann, M.; Mueller, W.; Sykora, J.; Kuhn, A.; et al. Yes and PI3K Bind CD95 to Signal Invasion of Glioblastoma. *Cancer Cell* **2008**, *13*, 235–248. [[CrossRef](#)] [[PubMed](#)]
18. Neumann, L.; Pforr, C.; Beaudouin, J.; Pappa, A.; Fricker, N.; Krammer, P.H.; Lavrik, I.N.; Eils, R. Dynamics within the CD95 death-inducing signaling complex decide life and death of cells. *Mol. Syst. Biol.* **2010**, *6*, 352. [[CrossRef](#)]
19. O’Reilly, L.A.; Tai, L.; Lee, L.; Kruse, E.A.; Grabow, S.; Fairlie, W.D.; Haynes, N.M.; Tarlinton, D.M.; Zhang, J.-G.; Belz, G.T.; et al. Membrane-bound Fas ligand only is essential for Fas-induced apoptosis. *Nature* **2009**, *461*, 659–663. [[CrossRef](#)] [[PubMed](#)]
20. Szaryńska, M.; Olejniczak, A.; Wierzbicki, P.; Kobiela, J.; Laski, D.; Sledzinski, Z.; Adrych, K.; Guzek, M.; Kmiec, Z. FasR and FasL in colorectal cancer. *Int. J. Oncol.* **2017**, *51*, 975–986. [[CrossRef](#)]
21. Peter, M.E.; Hadji, A.; Murmann, A.E.; Brockway, S.; Putzbach, W.; Pattanayak, A.; Ceppi, P. The role of CD95 and CD95 ligand in cancer. *Cell Death Differ.* **2015**, *22*, 549–559. [[CrossRef](#)]
22. Szaryńska, M.; Olejniczak, A.; Kobiela, J.; Łaski, D.; Śledziński, Z.; Kmiec, Z. Cancer stem cells as targets for DC-based immunotherapy of colorectal cancer. *Sci. Rep.* **2018**, *8*, 12042. [[CrossRef](#)]
23. Olejniczak, A.; Szaryńska, M.; Kmiec, Z. In vitro characterization of spheres derived from colorectal cancer cell lines. *Int. J. Oncol.* **2017**, *52*, 599–612. [[CrossRef](#)]
24. Chen, Z.; Li, W.; Qiu, F.; Huang, Q.; Jiang, Z.; Ye, J.; Cheng, P.; Low, C.; Guo, Y.; Yi, X.; et al. Aspirin cooperates with p300 to activate the acetylation of H3K9 and promote FasL-mediated apoptosis of cancer stem-like cells in colorectal cancer. *Theranostics* **2018**, *8*, 4447–4461. [[CrossRef](#)] [[PubMed](#)]
25. Dunbar, K.; Valanciute, A.; Lima, A.C.S.; Vinuela, P.F.; Jamieson, T.; Rajasekaran, V.; Blackmur, J.; Ochocka-Fox, A.-M.; Guazzelli, A.; Cammareri, P.; et al. Aspirin Rescues Wnt-Driven Stem-like Phenotype in Human Intestinal Organoids and Increases the Wnt Antagonist Dickkopf-1. *Cell. Mol. Gastroenterol. Hepatol.* **2021**, *11*, 465–489. [[CrossRef](#)]
26. Zhang, Y.; Lv, C.; Dong, Y.; Yang, Q. Aspirin-targeted PD-L1 in lung cancer growth inhibition. *Thorac. Cancer* **2020**, *11*, 1587–1593. [[CrossRef](#)] [[PubMed](#)]
27. Nath, S.; Devi, G.R. Three-dimensional culture systems in cancer research: Focus on tumor spheroid model. *Pharmacol. Ther.* **2016**, *163*, 94–108. [[CrossRef](#)]
28. Stankevicius, V.; Kunigenas, L.; Stankunas, E.; Kuodyte, K.; Strainiene, E.; Cicenias, J.; Samalavicius, N.E.; Suziedelis, K. The expression of cancer stem cell markers in human colorectal carcinoma cells in a microenvironment dependent manner. *Biochem. Biophys. Res. Commun.* **2017**, *484*, 726–733. [[CrossRef](#)]
29. Ahmed, D.; Eide, P.W.; Eilertsen, I.A.; Danielsen, S.A.; Eknæs, M.; Hektoen, M.; Lind, G.E.; Lothe, R.A. Epigenetic and genetic features of 24 colon cancer cell lines. *Oncogenesis* **2013**, *2*, e71. [[CrossRef](#)]
30. Tran Janco, J.M.; Lamichhane, P.; Karyampudi, L.; Knutson, K.L. Tumor-Infiltrating Dendritic Cells in Cancer Pathogenesis. *J. Immunol.* **2015**, *194*, 2985–2991. [[CrossRef](#)] [[PubMed](#)]
31. Qadir, A.S.; Stults, A.M.; Murmann, A.E.; Peter, M.E. The mechanism of how CD95/Fas activates the Type I IFN/STAT1 axis, driving cancer stemness in breast cancer. *Sci. Rep.* **2020**, *10*, 1310. [[CrossRef](#)]
32. Flanagan, L.; Meyer, M.; Fay, J.; Curry, S.; Bacon, O.; Duessmann, H.; John, K.; Boland, K.C.; McNamara, D.A.; Kay, E.W.; et al. Low levels of Caspase-3 predict favourable response to 5FU-based chemotherapy in advanced colorectal cancer: Caspase-3 inhibition as a therapeutic approach. *Cell Death Dis.* **2016**, *7*, e2087. [[CrossRef](#)]
33. Huang, Q.; Li, F.; Liu, X.; Li, W.; Shi, W.; Liu, F.-F.; O’Sullivan, B.; He, Z.; Peng, Y.; Tan, A.-C.; et al. Caspase 3-mediated stimulation of tumor cell repopulation during cancer radiotherapy. *Nat. Med.* **2011**, *17*, 860–866. [[CrossRef](#)] [[PubMed](#)]
34. Hadji, A.; Ceppi, P.; Murmann, A.E.; Brockway, S.; Pattanayak, A.; Bhinder, B.; Hau, A.; De Chant, S.; Parimi, V.; Kolesza, P.; et al. Death Induced by CD95 or CD95 Ligand Elimination. *Cell Rep.* **2014**, *7*, 208–222. [[CrossRef](#)]
35. Sladky, V.C.; Villunger, A. Uncovering the PIDDosome and caspase-2 as regulators of organogenesis and cellular differentiation. *Cell Death Differ.* **2020**, *27*, 2037–2047. [[CrossRef](#)] [[PubMed](#)]
36. Jaime-Sanchez, P.; Uranga-Murillo, I.; Aguilo, N.; Khouili, S.C.; Arias, M.A.; Sancho, D.; Pardo, J. Cell death induced by cytotoxic CD8 + T cells is immunogenic and primes caspase-3-dependent spread immunity against endogenous tumor antigens. *J. Immunother. Cancer* **2020**, *8*, e000528. [[CrossRef](#)]
37. Liu, J.; Wang, F.; Yin, D.; Zhang, H.; Feng, F. Caspase 3 may participate in the anti-tumor immunity of dendritic cells. *Biochem. Biophys. Res. Commun.* **2019**, *511*, 447–453. [[CrossRef](#)]
38. Yang, T.; Zhang, W.; Wang, L.; Xiao, C.; Wang, L.; Gong, Y.; Huang, D.; Guo, B.; Li, Q.; Xiang, Y.; et al. Co-culture of dendritic cells and cytokine-induced killer cells effectively suppresses liver cancer stem cell growth by inhibiting pathways in the immune system. *BMC Cancer* **2018**, *18*, 984. [[CrossRef](#)] [[PubMed](#)]
39. Li, S.; Dai, W.; Mo, W.; Li, J.; Feng, J.; Wu, L.; Liu, T.; Yu, Q.; Xu, S.; Wang, W.; et al. By inhibiting PFKFB3, aspirin overcomes sorafenib resistance in hepatocellular carcinoma. *Int. J. Cancer* **2017**, *141*, 2571–2584. [[CrossRef](#)]

40. Yan, K.-H.; Lee, L.-M.; Hsieh, M.-C.; Yan, M.-D.; Yao, C.-J.; Chang, P.-Y.; Chen, T.-L.; Chang, H.-Y.; Cheng, A.-L.; Lai, G.-M.; et al. Aspirin antagonizes the cytotoxic effect of methotrexate in lung cancer cells. *Oncol. Rep.* **2013**, *30*, 1497–1505. [[CrossRef](#)]
41. Yan, K.-H.; Yao, C.-J.; Chang, H.-Y.; Lai, G.-M.; Cheng, A.-L.; Chuang, S.-E. The synergistic anticancer effect of troglitazone combined with aspirin causes cell cycle arrest and apoptosis in human lung cancer cells. *Mol. Carcinog.* **2010**, *49*, 235–246. [[CrossRef](#)] [[PubMed](#)]